Field Compressing Magnetothermal Instability in Laser Plasmas

J. J. Bissell, C. P. Ridgers, and R. J. Kingham
The Blackett Laboratory, Imperial College London, SW7 2BZ, United Kingdom
(Received 13 January 2010; published 18 October 2010)

The mechanism for a new instability in magnetized plasmas is presented and a dispersion relation derived. Unstable behavior is shown to result purely from transport processes—feedback between the Nernst effect and the Righi-Leduc heat-flow phenomena in particular—neither hydrodynamic motion nor density gradients are required. Calculations based on a recent nanosecond laser gas-jet experiment [D. H. Froula *et al.*, Phys. Rev. Lett. **98**, 135001 (2007)] predict growth of magnetic field and temperature perturbations with typical wavelengths of order 50 μm and characteristic growth times of $\sim$0.1 ns. The instability yields propagating magnetothermal waves whose direction depends on the magnitude of the Hall parameter.

DOI: 10.1103/PhysRevLett.105.175001 PACS numbers: 52.25.Fi, 52.25.Xz, 52.35.−g

The existence of large self-generated magnetic fields in laser-produced plasmas ($\sim$ 100 T) has long been known [1,2]. These fields can significantly affect the distribution of thermal energy in plasma targets by suppressing the cross-field thermal conductivity [3]. In recent years several experiments have been designed to assess their impact on inertial confinement fusion (ICF) schemes [4] and to study more general magnetic phenomena in laser plasmas, such as magnetic reconnection [5] and instability [6]. In addition, there has been increased discussion of the possible uses for applied magnetic fields in the suppression of nonlocal transport [7], control of plasma density channels [8], wakefield acceleration [9] and magnetized target fusion (MTF) schemes [10].

In this Letter we report a new instability shown computationally to impact on magnetized plasmas, though it may also take effect in the presence of self-generated fields. The instability compresses the magnetic field and distorts thermal-energy profiles by concentrating the heat flow (see Fig. 1), and may be important when a high degree of symmetry or control of heat transport is needed, or where uniform fields are applied for a specific purpose, such as those cases mentioned above [7–10].

Feedback is driven solely by classical (Braginskii) transport processes [3], specifically the interaction of the Nernst effect, which describes advection of magnetic field with heat-flow down temperature gradients $\mathbf{q}_\perp$ and with velocity $\mathbf{v}_N \approx 2\mathbf{q}_\perp/5P_e$, where P_e is the isotropic pressure [11], and the Righi-Leduc heat-flow, the cross-field thermal-flux "bent" by magnetic fields acting on negatively charged heat-carrying electrons. Consequently, we require only the presence of temperature gradients ∇T_e perpendicular to an existing magnetic field for instability. Gradients in electron number density n_e are not needed (i.e., $\nabla n_e = \mathbf{0}$, precluding $\nabla T_e \times \nabla n_e$ field generation), nor hydrodynamic motion or anisotropic pressure. Thus, what we see is distinct from instabilities existing in the literature such as the field-generating thermal instability [12–14], for which $\nabla T_e \times \nabla n_e$ is necessarily nonzero; and those of Weibel [15], where magnetic fields are not essential; Haines [16,17], which does not require either Righi-Leduc heat flow or the Nernst effect; and Davies [18], where unstable filamentation arises from plasma motion.

In our case, terms responsible for growth go as $k^{3/2}$, where k is the wave number of a perturbation, yielding traveling waves rather than purely growing perturbations. These, however, differ from the thermal-magnetic waves described by Pert [19] who neglected the Nernst effect.

We present an analytical theory of the instability alongside results from numerical simulation in the context of an experimental arrangement which uses applied magnetic fields; specifically the conditions of Froula *et al.* [7], in

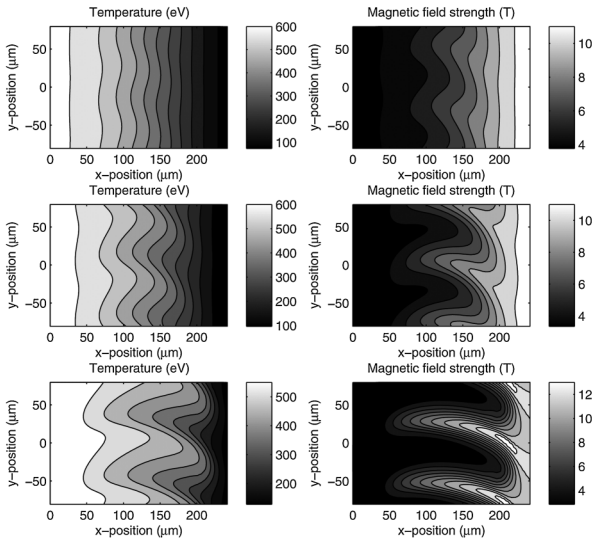

FIG. 1. Snapshots of the instability taken at 700 ps (top), 800 ps (center), and 900 ps (bottom), from CTC simulations of the experiment of Froula *et al.* [7] for the case of an 8 T field given a 1% perturbation at the laser "switch-on" time.

kinetic modeling of which it was first observed [20]. In this experiment, designed to measure the suppression of nonlocal heat transport by magnetic fields, a nitrogen gas-jet (atomic number $Z = 7$), with electron number density $n_e = 1.5 \times 10^{19}\,\mathrm{cm}^{-3}$ and initial temperature $T_e = 20$ eV, was subject to inverse bremsstrahlung heating for 1 ns by a long-pulse laser of wavelength 1054 nm and intensity $6.3 \times 10^{14}\,\mathrm{W\,cm}^{-2}$. Uniform magnetic fields of strengths up to 12 T were imposed parallel to the laser-heating beam and the radial heat-flow inferred. These parameters should be assumed throughout.

Though the instability was originally observed in kinetic simulations [20], no theory was derived and to this end a classical transport model better elucidates the physics of the problem. Data presented here are thus taken primarily from our classical transport code CTC. Where appropriate, however, we present results from our kinetic code IMPACT [21] and from CTC+: a version of CTC which includes hydrodynamic motion. For the conditions considered here, simulation using CTC+ reveals that neither hydrodynamics nor density gradients impact heavily on the instability (see Fig. 2), so that both effects are neglected in the theory at this stage.

For consistency with Froula *et al.* [7], we focus on a two-dimensional cross-section through a plasma perpendicular to both the applied magnetic field and the laser-heating beam. However, for simplicity we consider an x-y, rather than r-θ geometry, with a laser-heating strip resulting from a heating operator $\dot{U}_L(x)$ in place of a circular laser spot. We thus suppose a plasma with principal temperature and magnetic field gradients along the x axis of the system only. The magnetic field is applied parallel to the z axis, i.e., $\mathbf{B} = B\hat{\mathbf{z}}$, where $B = |\mathbf{B}|$, so that plasma scalar quantities f and vector quantities $\mathbf{A}$ are such that $\mathbf{B} \cdot \nabla f = \mathbf{B} \cdot \mathbf{A} = 0$. Snapshots of the instability in this geometry are shown in Fig. 1.

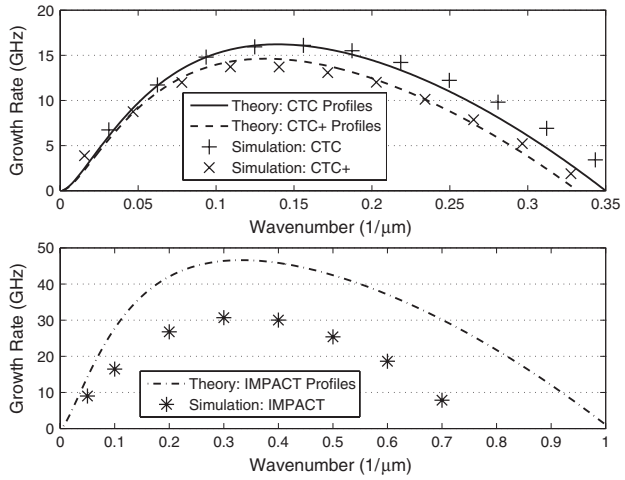

FIG. 2. The theoretical dispersion relation of our reduced model—for a 6 T magnetized plasma at a distance $x \approx 120\ \mu$m from the laser strip center after 500 ps of heating—based on one-dimensional profiles taken from CTC (top plot, solid line), CTC+ (top plot, dashed line) and IMPACT (bottom plot). These may be compared with growth rates measured from full two-dimensional simulations.

Our transport code incorporates the full Braginskii model with corrected coefficients [3,22,23]. However, the theory presented here includes just the most important damping terms, resistive and thermal diffusion, alongside the main feedback terms describing the Nernst effect and Righi-Leduc heat flow. The Ettingshausen term, which helps to mitigate diffusive effects, is also retained. In this way, using Braginskii's expression for the electric field $\mathbf{E}$ and Ampère's Law to write the current as $\mathbf{j} = (\nabla \times \mathbf{B})/\mu_0$, and by neglecting hydrodynamics and density gradients ($\nabla n_e = \mathbf{0}$), the induction equation is

$$\frac{\partial \mathbf{B}}{\partial t} = -\nabla \times \mathbf{E} = -\nabla \times \left(\frac{m_e \alpha_\perp}{e^2 n_e c_B \tau_T \mu_0} \nabla \times \mathbf{B} - \frac{\beta_\wedge}{e} \hat{\mathbf{z}} \times \nabla T_e \right). \quad (1)$$

Similarly, by neglecting Ohmic heating, using Braginskii's form for the heat flow $\mathbf{q}$, and with a laser-heating operator $\dot{U}_L(x)$, the thermal-energy continuity equation of our reduced model becomes

$$\frac{3}{2} n_e \frac{\partial T_e}{\partial t} = -\nabla \cdot \mathbf{q} + \dot{U}_L = \nabla \cdot \left(\frac{n_e c_B \tau_T T_e}{m_e} [\kappa_\perp \nabla T_e + \kappa_\wedge \hat{\mathbf{z}} \times \nabla T_e] \right) + \nabla \cdot \left(\frac{T_e}{e \mu_0} \psi_\wedge \hat{\mathbf{z}} \times (\nabla \times \mathbf{B}) \right) + \dot{U}_L. \quad (2)$$

In these equations e is the electronic charge, $c_B = 3\sqrt{\pi}/4$ is a dimensionless constant, and the thermal collision time $\tau_T = 4\pi v_T^3 / n_i [Ze^2/\epsilon_0 m_e]^2 \ln\Lambda_{ei}$ is defined by the thermal velocity $v_T = (2T_e/m_e)^{1/2}$, the ion number density $n_i \approx n_e/Z$ and the Coulomb logarithm $\ln\Lambda_{ei} \approx 8$. The transport coefficients—the resistivity $\alpha_\perp$, thermal conductivity $\kappa_\perp$, Nernst, Ettingshausen, and Righi-Leduc terms, $\beta_\wedge$, $\psi_\wedge$, and $\kappa_\wedge$ respectively—are dimensionless functions of the atomic number Z and Hall parameter $\chi = \omega_g c_B \tau_T$ only, where $\omega_g = eB/m_e$ is the electron gyrofrequency. These are calculated using polynomial fits in the Lorentz approximation [22,23].

Taking zeroth order solutions to Eqs. (1) and (2) of the form $B = B_0(x, t)$ and $T_e = T_0(x, t)$, we add wavelike perturbations with wave number k and frequency ω at an (anticlockwise) angle θ to the x axis. In this way we have $T_e = T_0 + \delta T$ and $B = B_0 + \delta B$, where $\delta T = \delta T' \exp i(k_x x + k_y y - \omega t)$, $\delta B = \delta B' \exp i(k_x x + k_y y - \omega t)$, $k_x = k\cos\theta$, $k_y = k\sin\theta$, and $\delta T'$, and $\delta B'$ are complex. Hence, by defining temperature and magnetic field scale lengths $L_T = T_0/(\partial T_0/\partial x)$ and $L_B = B_0/(\partial B_0/\partial x)$ respectively, and assuming $|kL_{T,B}| \gg 1$ and $|\nabla(1/L_{T,B})| \lesssim 1/L_{T,B}^2$, the first order forms of Eqs. (1) and (2) yield a quadratic in ω and the dispersion relation

$$\omega_{\pm} = \tfrac{1}{2}\{s_B k - (d_R + d_T)ik^2\} \pm \tfrac{1}{2}\{s_B^2 k^2 + [s_P + 2s_B \times (d_R - d_T)]ik^3 - [(d_R - d_T)^2 + s_E]k^4\}^{1/2}. \quad (3)$$

Here the additional d and s coefficients are defined in terms of the mean free path $\lambda_T = \tau_T v_T$ and the skin depth $\delta = c/\omega_{\rm pe}$, where c is the speed of light and $\omega_{\rm pe} = (e^2 n_e/m_e\epsilon_0)^{1/2}$ is the plasma frequency

$$s_P = \frac{2\beta_\wedge c_B^2 \lambda_T^4}{3L_T\tau_T^2}\frac{\partial\kappa_\wedge}{\partial\chi}\sin\theta, \qquad s_B = \frac{c_B\chi\lambda_T^2}{3L_B\tau_T}\frac{\partial\kappa_\wedge}{\partial\chi}\sin\theta,$$
$$s_E = \frac{4\lambda_T^2\delta^2}{3\tau_T^2}\beta_\wedge\psi_\wedge, \qquad d_R = \frac{\alpha_\perp\delta^2}{c_B\tau_T}, \quad \text{and} \quad d_T = \frac{c_B\kappa_\perp\lambda_T^2}{3\tau_T}.$$

Note that d_R and d_T represent the coefficients for resistive and thermal diffusion, respectively. The solution for ω_+ yields unstable modes for a range of k up to a cutoff k_c with growth rates given by $\Im\{\omega_+\}$ (see Fig. 2), though the local approximation subjects us to the additional restriction $|1/L_{T,B}| \ll |k| \ll 1/\lambda_T$.

Perturbations grow primarily as a result of interplay between the Nernst effect and the Righi-Leduc heat-flow in the s_P source term in Eq. (3), yielding growth that goes as $k^{3/2}$; while the main damping terms in d_R and d_T are proportional to k^2, giving us the form of the dispersion curve in Fig. 2 (the term in s_B also contributes as a source, but is not essential). The angular dependence of s_B and s_P means that a y component to the perturbation is needed for instability. In our simulations, and hereafter in this Letter, we take $\theta = \pi/2$, i.e., $\sin\theta = 1$. Feedback between the Nernst and Ettingshausen effects, which goes like k^2 and is accounted for by s_E, acts to reduce the impact of diffusion, but cannot itself drive instability due to its equivalent power in k. Thus, the instability is perhaps best understood by assessing the phenomena in the principal source term s_P.

The effect of a temperature perturbation on an unperturbed magnetic field ($B = B_0$) may be considered by examining the first order correction due to the Nernst term in the induction equation:

$$\left(\frac{\partial B}{\partial t}\right)^{\rm O(1)}_{\beta_\wedge} = \frac{\beta_\wedge}{e}k^2\delta T e^{i\pi}. \quad (4)$$

Hence, a magnetic field perturbation is induced in antiphase. Physically, this is a result of the compressional aspect of Nernst advection. The Nernst velocity—the velocity of advection—is proportional to $-\partial T_e/\partial y$, so that the magnetic field is compressed in the troughs of the temperature perturbation and rarefacted at the peaks.

Similarly, we consider the impact of a magnetic field perturbation on an unperturbed temperature profile ($\partial T_0/\partial x < 0$) using the first order correction due to the Righi-Leduc term in the energy continuity equation:

$$\left(\frac{\partial T}{\partial t}\right)^{\rm O(1)}_{\kappa_\wedge} \propto \frac{\partial T_0}{\partial x}\frac{\partial\kappa_\wedge}{\partial\chi}k\delta B e^{i(\pi/2)}. \quad (5)$$

For χ greater than about 10^{-1} we have $\partial\kappa_\wedge/\partial\chi < 0$, in which case the magnetic field perturbation will induce a temperature perturbation that leads by $\pi/2$. This is due to the dependence of $\kappa_\wedge$ on χ, which is itself directly proportional to B. Since $\partial\kappa_\wedge/\partial\chi < 0$, regions of higher magnetic field strength have a lower Righi-Leduc heat-flow, so that heat is transported away from these regions more slowly than those of lower B. Thus, as we move along the positive y axis, thermal energy is built up in places where heat flow goes from high to low and removed from places where it goes from low to high. The reverse is found if χ is less than about 10^{-1}, where $\partial\kappa_\wedge/\partial\chi > 0$.

The two stages of this feedback process result in induced perturbations which have different phases. Magnetic field perturbations will tend to "push" temperature perturbations towards a phase difference of $\pm\pi/2$ (sign identical to that of $[\partial T_0/\partial x][\partial\kappa_\wedge/\partial\chi]$), while temperature perturbations "pull" magnetic field perturbations towards a phase of π. The net result of this "push-pull" interaction is that perturbations propagate as waves with a phase difference of $\phi \approx 3\pi/4$ and in the direction $\pm\hat{\mathbf{y}}$ (again, sign identical to that of $[\partial T_0/\partial x][\partial\kappa_\wedge/\partial\chi]$).

The dependence of the d and s coefficients on $T_0(x, t)$ and $B_0(x, t)$ means that the growth rate varies both temporally and spatially. Evaluation of the dispersion relation is thus limited to a particular plasma cross section x and based on a given snapshot of the bulk profile. When using profiles taken from computational simulation of the experiment of Froula *et al.* [7], the theoretical model and growth rates measured from full heating simulations show good agreement (see Fig. 2).

As indicated in Fig. 2, for the conditions considered here hydrodynamics does not significantly affect the instability. Nonlocal effects, on the other hand, which are relevant to the experiment of Froula *et al.* [7], do reduce the predictive power of the theory by modifying the transport coefficients; though the physical mechanism of the instability remains the same. However, simulation using IMPACT (see Fig. 2) shows that this reduction is not dramatic: the peak wave number is effectively unchanged, while the cutoff wave number and peak growth rate agree to within ~35%. Indeed, it is noteworthy that though growth rates measured from kinetic simulations are lower than those predicted by the theory, the different bulk profiles mean that rates are approximately twice those taken from CTC and CTC+.

The cutoff wave number for unstable modes k_c, calculated by solving $\Im\{\omega_+\} = 0$, may be expressed in terms of the dimensionless parameters χ and $\Lambda = (\lambda_T/\delta)$:

$$k_c L_T = \frac{c_B}{3}\frac{\partial\kappa_\wedge}{\partial\chi}\left(\frac{3}{\alpha_\perp\kappa_\perp - \beta_\wedge\psi_\wedge}\right)^{1/2}\left(\frac{\beta_\wedge}{2} - \frac{\kappa_\perp\chi}{3}\frac{L_T}{L_B}\right)^{1/2} \times\left(\alpha_\perp\chi\frac{L_T}{L_B} + \frac{\beta_\wedge c_B^2}{2}\Lambda^2\right)^{1/2}\left(\frac{\alpha_\perp}{c_B\Lambda^2} + \frac{c_B\kappa_\perp}{3}\right)^{-1}. \quad (6)$$

This equation makes clear the necessity of both the Nernst effect and Righi-Leduc heat-flow in driving

instability: without the former ($\beta_\wedge = 0$), k_c becomes imaginary, and without the latter ($\partial\kappa_\wedge/\partial\chi = 0$), k_c is zero. It also demonstrates how feedback between the Nernst and Ettingshausen effects reduces the impact of the diffusive term in $\alpha_\perp\kappa_\perp$—thus extending the range of instability.

No equivalent expression for the peak wave number k_M exists; however, for the experiment of Froula *et al.* [7] we find $|s_B^2 - [(d_R - d_T)^2 + s_E]k_M^2| \approx |[s_P + 2(d_R - d_T)s_B]k_M|$, so that the peak growth rate γ_M and wave number k_M may be approximated by γ'_M and k'_M respectively, where

$$\gamma'_M = \tfrac{1}{2}[s_P + 2(d_R - d_T)s_B]^{1/2}k_M'^{(3/2)} - \tfrac{1}{2}(d_R + d_T)k_M'^2 \quad (7)$$

and

$$k'_M = \tfrac{9}{16}[s_P + 2(d_R - d_T)s_B][d_R + d_T]^{-2}. \quad (8)$$

More precise values for both γ_M and k_M may be found computationally under the assumption $L_T \approx -L_B$. Using $\Lambda = 20$ (characteristic for the experiment of Froula *et al.* [7]) and by comparing these values with γ'_M and k'_M, we find that the approximate expressions agree to within a factor of 5 for $10^{-2} < \chi < 10^2$.

To enable more qualitative discussion, we simplify further by assuming no magnetic field gradients ($L_B \to \infty$), so that $s_B = 0$, take $\Lambda \gg \max\{1, \chi\}$, for which $d_T \gg d_R$, and combine Eqs. (7) and (8) to express the peak growth rate as $\gamma'_M = (3/8)^3 s_P^2 d_T^{-3}$, i.e., $\gamma'_M\tau_T \approx [(\beta_\wedge\lambda_T/L_T) \times (\partial\kappa_\wedge/\partial\chi)]^2\kappa_\perp^{-3}$. Writing γ'_M in this way emphasizes the importance of steep temperature gradients, through $1/L_T^2$, and of intermediate Hall parameter, to allow significant $\beta_\wedge^2(\partial\kappa_\wedge/\partial\chi)^2/\kappa_\perp^3$. More specifically, we require χ in the region of 10^{-2} to 10^2, but avoiding $\chi \sim 10^{-1}$ where $\partial\kappa_\wedge/\partial\chi \sim 0$. Furthermore, the dimensionless form indicates relevance to other plasmas in self-similar regimes.

Under the conditions considered in this letter, the instability has growth rates of order 10 GHz, optimal wavelengths of $\sim$50 μm and can significantly disrupt magnetic field and temperature profiles over nanosecond time scales when compared to stable heating simulations. By concentrating the heat-flow in regions where the magnetic field is rarefacted, the instability enhances the spread of thermal energy (see Fig. 3).

To conclude, we have derived the linear theory for a new plasma instability in magnetized plasmas, which predicts propagating waves with growing amplitude for a range of wave numbers, and have shown that this theory compares well with simulation. Uniquely, the instability results solely from feedback between collisional transport processes, principally the Nernst effect and Righi-Leduc heat flow; though further investigation of the effects of hydrodynamics and nonlocal heat flow are key areas of future work. The instability is likely to be important for ICF (particularly hohlraum gas-fill conditions which are similar to those considered here) and most likely MTF. Furthermore, its existence highlights the necessity of including the Nernst effect and Righi-Leduc heat-flow in magneto-hydrodynamic models for any plasma of intermediate magnetization.

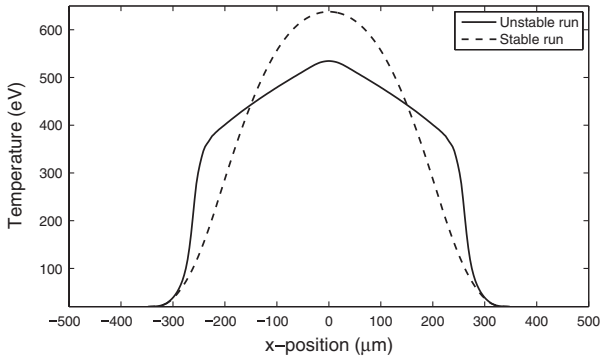

FIG. 3. A comparison between the spread of thermal energy when the instability is active (solid line) and when it is not (dashed line) after 1 ns of laser heating for the case of an 8 T applied field (cf. Fig. 1). The data, taken from CTC, are averaged in y for each x cross section.

We would like to acknowledge useful discussions with Dr A. G. R. Thomas. This work was funded by the UK Engineering and Physical Sciences Research Council (Grant No. EP/P502500/1).

[1] J. A. Stamper *et al.*, Phys. Rev. Lett. **26**, 1012 (1971).
[2] A. Raven, O. Willi, and P. T. Rumsby, Phys. Rev. Lett. **41**, 554 (1978).
[3] S. I. Braginskii, in *Reviews of Plasma Physics* Vol. I, edited by M. A. Leontovich (Consultants Bureau, New York, 1965), p. 205.
[4] P. M. Nilson *et al.*, Phys. Rev. Lett. **97**, 255001 (2006).
[5] C. K. Li *et al.*, Phys. Rev. Lett. **99**, 055001 (2007).
[6] C. K. Li *et al.*, Phys. Rev. Lett. **99**, 015001 (2007).
[7] D. H. Froula *et al.*, Phys. Rev. Lett. **98**, 135001 (2007).
[8] D. H. Froula *et al.*, Plasma Phys. Controlled Fusion **51**, 024009 (2009).
[9] T. Hosokai *et al.*, Phys. Rev. Lett. **97**, 075004 (2006).
[10] I. R. Lindemuth *et al.*, Phys. Rev. Lett. **75**, 1953 (1995).
[11] A. Nishiguchi, T. Yabe, and M. G. Haines, Phys. Fluids **28**, 3683 (1985).
[12] D. Tidman and R. Shanny, Phys. Fluids **17**, 1207 (1974).
[13] M. Ogasawara, A. Hirao, and H. Ohkubo, J. Phys. Soc. Jpn. **49**, 322 (1980).
[14] A. Hirao, J. Phys. Soc. Jpn. **50**, 668 (1981).
[15] E. S. Weibel, Phys. Rev. Lett. **2**, 83 (1959).
[16] M. G. Haines, J. Plasma Phys. **12**, 1 (1974).
[17] M. G. Haines, Phys. Rev. Lett. **47**, 917 (1981).
[18] J. R. Davies *et al.*, Plasma Phys. Controlled Fusion **51**, 035013 (2009).
[19] G. J. Pert, J. Plasma Phys. **18**, 227 (1977).
[20] C. P. Ridgers, R. J. Kingham, and A. G. R. Thomas, Phys. Rev. Lett. **100**, 075003 (2008).
[21] R. J. Kingham and A. R. Bell, J. Comput. Phys. **194**, 1 (2004).
[22] E. M. Epperlein and M. G. Haines, Phys. Fluids **29**, 1029 (1986).
[23] C. P. Ridgers *et al.*, Phys. Plasmas **15**, 092311 (2008).